



Evaluation of Transcritical Rankine Cycle Driven by Low-Temperature Geothermal Source for Different Supercritical Working Fluids

Önder KIZILKAN*¹

¹Isparta University of Applied Sciences, Faculty of Technology, Department of Mechanical Engineering, Isparta, Turkey

(Alınış Tarihi/Received: 06.09.2019, Kabul Tarihi/Accepted: 23.11.2019)

*İlgili yazar/Corresponding Author: onderkizilkan@isparta.edu.tr

Keywords

Geothermal energy
Transcritical Rankine cycle
Supercritical fluid
Exergy

Abstract: Turkey's energy consumption has risen in conjunction with its economic growth over the past decades. However, approximately 70 % of the electricity demand is supplied by fossil-based fuels, which are mainly imported from other countries. Thus, it became very important for the country to find alternative ways of meeting the energy requirement. Due to its geographical position, the renewable energy potential of Turkey is fairly well, which is currently contributing to the energy generation but not at the desired level. One of them is the geothermal energy that Turkey has many geothermal areas, and they are relatively appropriate for electricity production. This study aims to investigate the performance of a geothermal based transcritical Rankine cycle for various supercritical working fluids. The geothermal reservoir is located in the west part of Turkey, and the geothermal water temperature is about 156 °C. Using the actual data, comparative thermodynamic analyses are carried out for determining the best working fluid. Results show that the highest power generation rate is calculated for the cycle using R170 with 6125 kW, followed by R744. In addition, the highest irreversibility is calculated for R125 with an exergy destruction rate of 8397 kW.

Düşük Sıcaklıklı Jeotermal Kaynak ile Çalışan Transkritik Rankine Çevrimin Farklı Süperkritik Akışkanlar için Değerlendirilmesi

Anahtar Kelimeler

Jeotermal enerji
Transkritik Rankine çevrimi
Süperkritik akışkan
Ekserji

Özet: Türkiye'nin enerji tüketimi son yıllarda ekonomik büyümeye paralel olarak artış göstermiştir. Bununla beraber, elektrik ihtiyacının % 70'i diğer ülkelerden ithal edilen fosil kaynaklı yakıtlardan sağlanmaktadır. Bu nedenle, ülkemizin enerji gereksinimi için alternatif yolların bulunması büyük önem arz etmektedir. Coğrafi konumu dolayısıyla ülkemizin yenilenebilir enerji potansiyeli oldukça iyidir. Hâlihazırda, yeterince olmasa bile ülkemizde yenilenebilir kaynaklardan enerji üretimi hızla artmaktadır. Bunlardan birisi, hem ülkemizde birçok yerde bulunan ve hem de elektrik üretimi için uygun olan jeotermal enerjidir. Bu çalışmanın amacı, jeotermal enerji ile çalışan transkritik Rankine çevriminin farklı süperkritik akışkanlar için performansının incelenmesidir. Jeotermal kaynak, ülkemizin batısında yer almaktadır ve jeotermal su sıcaklığı 156 °C'dir. Aktif olarak çalışan bir santralden alınan veriler kullanılarak en uygun iş akışkanının belirlenmesi için kıyaslamalı termodinamik analizler yapılmıştır. Sonuçlara göre, en yüksek güç üretimi, 6125 kW ile R170 akışkanının kullanıldığı çevrimde gerçekleştirilmiştir. R170 akışkanı R744 takip etmektedir. Bunun yanında, en yüksek tersinmezlik değeri 8397 kW ile R125 akışkanı için hesap edilmiştir.

1. Introduction

It is important to support the penetration of renewables to mitigate climate change and to improve the cycle efficiencies of renewable and non-renewable technologies. Heat engines using low-temperature resources have inherently low conversion efficiencies. At temperatures below 400 °C, organic Rankine cycles (ORC) are the most effective at extracting power from low-temperature sources such as geothermal, waste heat, and biomass sources (Moloney et al., 2017). Within the low-temperature sources, geothermal resources are promising energy sources that can reduce pollutant emissions and fossil fuel consumption. According to the International Energy Agency, 3.5% of the worldwide generated power is expected to be generated by geothermal energy by 2050 (Sun et al., 2018). Geothermal energy resources of low and medium enthalpy are available in countries like Turkey, Italy, Indonesia, or the United States. For these kinds of resources, binary cycles like the Organic Rankine Cycle (ORC) are suitable as energy conversion systems (Heberle et al., 2017a; 2017b).

As a waste heat recovery technology, ORC is widely used in industrial waste heat, solar energy, geothermal energy and other fields due to its wide range of recoverable heat sources, low maintenance costs, favorable operating pressure and autonomous operation (Zhang et al., 2019). Also, ORCs have been developed to generate electricity over the past two decades as an efficient method for such resources. Nevertheless, geothermal ORC system efficiencies are still less than 12% for moderate-low temperature geothermal energy sources (below 150 °C) due to the limited temperature difference between the heat source and sink. Most efforts in the literature have sought to maximize the ORC thermodynamic efficiencies by improving the system configurations and selecting the best working fluids, including pure organic fluids or zeotropic mixtures (Sun et al., 2018).

The performance of ORCs significantly depends on the working fluid. It is still challenging to establish a universal ORC working fluid selection criteria since the application consists of a combination of thermal performance, cost, and environmental impact with different heat source conditions. The ORC power generation system performance is highly sensitive to the available energy potential of the heat source, which also determines the ORC power generation system configuration and the working fluid used (Wang et al., 2019). Many studies have examined the influence of the properties of the single ORC component working fluids as well. Song et al. (2019) investigated a trans-critical ORC for 52 different working fluids in order to analyze the effect of fluid dryness and critical temperature on the power cycle. This study is probably the most comprehensive research conducted for the working fluids. Ganjehsarabi (2019), performed thermodynamic and economic analyses for an ORC with proton exchange membrane electrolyzer. The analyses were carried out for a mixture of butane, pentane, and iso-pentane as working fluids. Xu et al. (2019) investigated the ORC working with zeotropic fluids to evaluate the performance improvement of the system. Yu et al. (2019), evaluated the performance of an ORC for 22 working fluids. In the results, it was reported that the most energy-efficient fluids were R125, R143a, R290 and R1270 for without waste heat utilization and R170, R134a, and R290 for with utilizing waste heat. Thurairaja et al. (2019), examined the performance of an ORC for different working fluids. They performed the analyses for different temperature ranges using around 100 working fluids which were suitable for ORCs. From the literature, some common refrigerants used in ORCs depending on the temperature of the heat source are given in Table 1 (Kajurek et al., 2019).

Table 1. Recommended refrigerants (Kajurek et al., 2019)

Source temperature [°C]	Recommended refrigerant
<100	R32, R125, R134a, R143a,
100–120	R124, R227ea, R290, R1234yf, R1270
120–160	R114, R141b, R123, R124, R245fa, R601a, R1243ze
160–200	R123, R141b, R1234ze, RC218, R236fa, R236ea, R600, R601
>200	benzene, paraxylene, toluene, hexane

For the last decades, there is a large volume of published studies on geothermal based thermodynamic cycles using different working fluids and different cycle configurations. Wang et al. (2019), studied the working fluid selection criteria for a power plant which was assisted supercritical carbon dioxide (sCO₂) from a geothermal reservoir. They investigated fluid behaviors in order to determine the most feasible ORC design. Abdolalipouradl et al. (2019) investigated the geothermal power plant performance in terms of thermodynamics and exergoeconomics. In the analysis, a comparison with Kalina cycle and ORC working with CO₂. Li et al. (2018), presented a quantitative performance analysis for the off-design operation of tCO₂ system powered by geothermal energy. Another study was performed for the thermodynamic analysis of the geothermal energy assisted ORC by Karimi and Mansouri (2018) for R600a, R601a, R152a, R134a, R11, R123. Nami et al. (2007), performed advanced exergy analysis for the performance evaluation of a geothermal driven dual fluid organic

Rankine cycle working with isopentane and isobutene. Fiaschi et al. (2017), analyzed thermodynamically geothermal based ORC and KC for comparison purposes. For the ORC, R245fa, Isobutene, R600, R218, transcritical CO₂ (tCO₂), sCO₂, R1234ze, R1233zd, R404a, r407c, n-octane, and n-pentane. Yang et al., (2017) investigated the ORC working with R245fa driven by geothermal resource from abandoned oil wells.

From the recent literature, it can be seen that a considerable amount has been published on the performance of the geothermal ORCs for several working fluids. However, studies on power generation using supercritical fluids are limited. Furthermore, there is no comprehensive research that focuses specifically on supercritical working fluids. In this study, it is aimed to investigate the performance of the geothermal Rankine cycle for different supercritical working fluids: carbon dioxide, ethane, fluoromethane, pentafluoroethane, and sulfur hexafluoride. For the energetic and exergetic analysis, a basic transcritical Rankine cycle is driven by geothermal power. The performance of the power cycle is evaluated for different fluids, comparatively. In addition, a parametric study is conducted for determining the effects of turbine inlet pressure and temperature on the system performance.

2. Selection of Working Fluids

The selection of the working fluid plays a key role in the ORC process and is determined by the grade of heat source temperature, ambient temperature or coolant liquid temperature and other criteria. Although high system efficiency is the main goal when designing heat recovery systems, one has to take into account the environmental characteristics for safety and practical considerations. For example, as the HCFCs still contain chlorine and have an associated Ozone Depletion Potential, they will be phased out in the EU Community from the 1st of January 2010. So, the availability of HCFCs for equipment servicing following the phase-out may not allow for predictable, economical use (Jumel et al., 2012; Bandean et al., 2011). A suitable fluid for an ORC has to fulfill several requirements. Desirable properties include low specific volumes, high efficiency, moderate pressures, low cost, low toxicity, low ozone depletion potential (ODP), and low global warming potential (GWP). The latter is particularly important as with continuous efforts to reduce greenhouse gas emissions many high GWP fluids are being banned and phased out. Finally, safety reasons like the maximum allowable concentration and the explosion limit should be considered (Radulovic, 2015; Karellas and Schuster, 2008).

Working fluids for ORCs can be classified based on the slope of their saturated vapor curves as dry fluid, isentropic fluid, and wet fluid (Figure 1). A method used to determine the type of working fluids was first proposed by Liu et al. (2004). The measure of wetness or dryness of a fluid is measured by the inverse of the slope, defined as; $\xi = ds/sT$. Therefore, the value of $\xi > 0$ implies a dry fluid, $\xi \approx 0$ implies an isentropic fluid, and $\xi < 0$ implies a wet fluid (Babatunde and Sunday, 2018).

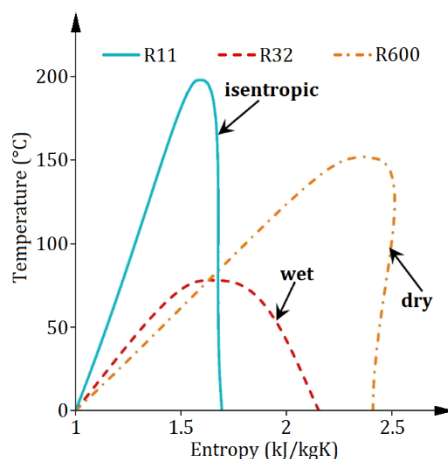


Figure 1. Three types of organic working fluids (reproduced from Wang et al., 2019)

Dry fluids are high molecular mass organic fluids exhibiting a positive slope on the T-s diagram. Wet fluids are low molecular mass organic fluids exhibiting negative slopes on the T-s diagram. Isentropic fluids are generally of medium molecular mass, exhibiting infinite or nearly vertical on the T-s diagram. Hence, wet fluids normally require superheating. Isentropic and dry fluids have been widely proposed for subcritical ORC basically to avoid the formation of the liquid droplet. For supercritical Rankine cycles utilizing wet or dry fluids, the turbine intake temperature must be sufficiently high to avoid the double phase region. If the temperatures are sufficiently high, the expansion process does not go through the double phase state; on the contrary, wet fluids are less affected by superheating after the expansion (Babatunde and Sunday, 2018).

While most commercial ORC plants exhibit a simple architecture: sub-critical working conditions, single-component working fluids, single evaporation pressure, and possible use of a recuperator heat exchanger, the use of fluids with low critical temperatures, even when low-temperature sources are employed, offers the possibility for the cycle to operate at supercritical conditions. Schuster et al. (2010) reported improved exergetic efficiency of the supercritical ORC. Supercritical ORC operation bypasses the liquid-vapor boundary, which results in an improved thermal match between the source and the fluid, which allows for more effective heat utilization. Thus, irreversibilities are lower, and exergy destruction is reduced (Radulovic, 2015).

The critical temperature is a function of the strength of the intermolecular interactions that bind the molecules of a substance together as a liquid, but it sets a limit on the evaporation temperature in subcritical cycles and also determines the temperature glide in zeotropic mixtures. Low critical temperature fluids perform better for supercritical cycles, however, the chemical stability of organic working fluids operating on supercritical cycle also depends on their critical temperatures because of the tendency to degenerate with a high degree of superheat (Babatunde and Sunday, 2018).

The first step when designing a transcritical Rankine cycle is the choice of the appropriate working fluid. According to the critical pressure and temperature, as well as the boiling temperature in various pressures (Karellas and Schuster, 2008), five supercritical working fluids have been selected for the analysis. As can be seen from Table 2, all the supercritical fluids selected for the present study have low critical temperatures, between 30-66 °C. The fluids are tabulated according to the order of rising critical temperature, T_c . All the fluids are wet type fluids except sulfur hexafluoride; it is an isentropic fluid.

Table 2. Properties of supercritical fluids studied (ASHRAE, 2009)

Working fluid	ODP	GWP	T_c (°C)	P_c (kPa)
Carbon dioxide (R744)	0	1	30.978	7377
Ethane (R170)	0	6	32.17	4872
Fluoromethane (R41)	0	92	44.13	5897
Sulfur hexafluoride (SF6)	0	22800	45.57	3755
Pentafluoroethane (R125)	0	3500	66.023	3617

3. Geothermal Driven Transcritical Power Cycle

The schematic representation of the geothermal driven transcritical Rankine cycle is shown in Figure 2. The geothermal reservoir is located in the west part of Turkey, and the geothermal water temperature is about 156 °C and extracted at 940 kPa with a mass flow rate of 165 kg/s. In addition, the reinjection temperature is 78.4 °C. The transcritical Rankine cycle consists of four main components, a turbine, vaporizer, condenser, and a pump. The superheated vapor needs to be cooled to a saturated liquid before entering the feed pump. For this aim, the condenser is connected to a cooling tower. In addition, there is a geothermal water loop extracted from the well and passes through the vaporizer where it rejects some amount of its thermal energy to the supercritical fluid.

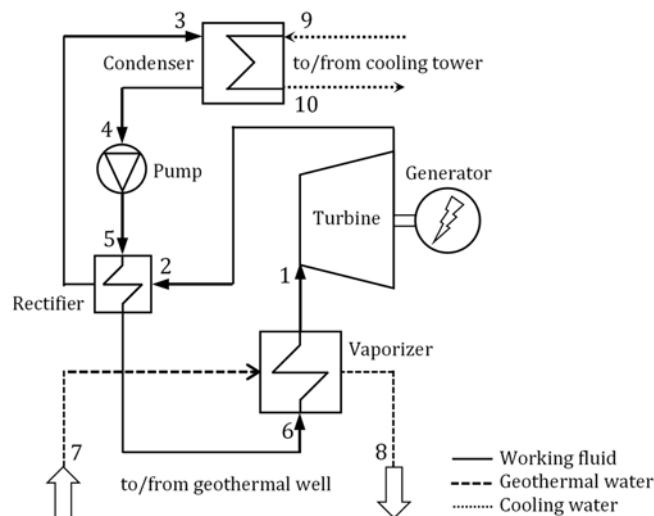


Figure 2. Schematic representation of geothermal driven transcritical Rankine cycle

For low-grade thermal energy utilization such as geothermal energy, the transcritical power generation cycle is relatively advantageous than the ORC. The temperature profile for the supercritical fluid above the critical point matches the geothermal source temperature profile better than a working fluid processed below the critical point. Accordingly, the problem which may occur in an ORC's heat exchanger (the so-called pinching problem), can be refrained by the transcritical cycle. This situation is illustrated in Figure 3 with the T-s diagram of the transcritical cycle (Chen et al., 2006).

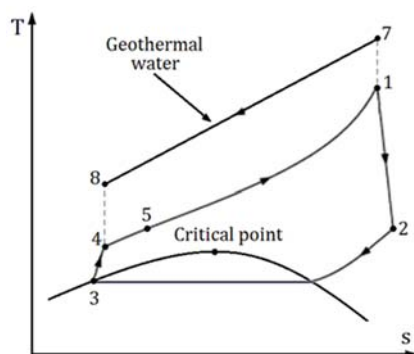


Figure 3. T-s diagram of transcritical Rankine cycle (reproduced from Wang et al., 2010)

For the performance analysis of the geothermal power plant for different supercritical fluids, the design parameters are tabulated in Table 3.

Table 3. Design parameters

Parameter	Value
Geothermal water temperature, T_7	156 °C
Reinjection temperature	78.4 °C
Mass flow rate of geothermal water	165 kg/s
Turbine inlet temperature, T_1	146 °C
Condenser saturation temperature, T_3	$T_c - 6$ °C
Pressure ratio, P_1/P_2	1.5
Cooling water temperature	$T_{wb} + 6$ °C
Mass flow rate of cooling water	1180 kg/s
Turbine isentropic efficiency, $\eta_{is,T}$	0.85 ^a
Pump isentropic efficiency, $\eta_{is,P}$	0.80 ^b
Heat exchanger effectiveness, ϵ	0.80 ^c
Minimum pinch point temperature	8 °C ^d

^a Meng et al. (2019),

^b Ahmedi et al. (2017)

^c Chen et al. (2005)

^d Thanganadar et al. (2019)

4. Methodology

A thermodynamic model is constructed using Engineering Equation Solver (EES) software (Klein, 2018) in order to evaluate the energetic and exergetic performance of the geothermal powered transcritical Rankine cycle for different working fluids. For the analyses, the following assumptions are made:

- All the processes are in steady-state and steady-flow conditions.
- The pressure drops throughout the cycle are neglected.
- Heat losses to/from the cycle are neglected.
- All the heat exchangers are counter flow type.
- The turbine and pump operations are assumed to be adiabatic.
- The geothermal fluid is assumed to be pure water without any solutes.
- Pump operations for the cooling tower and geothermal water extraction are neglected.
- Dead state temperature and pressure are taken as 18°C and 101.325 kPa, respectively.

The mass balance equation for steady-state and steady-flow processes can be written as (Cengel and Boles, 2006);

$$\sum \dot{m}_{in} = \sum \dot{m}_{out} \quad (1)$$

Here, \dot{m} is the mass flow rate, and the subscript in denotes inlet and out denotes outlet. The energy balance is expressed as:

$$\dot{Q} + \sum \dot{m}_{in}h_{in} = \dot{W} + \sum \dot{m}_{out}h_{out} \quad (2)$$

where \dot{Q} is the heat transfer rate, \dot{W} is the work, and h is the specific enthalpy. For the exergy analysis, the balance equation is defined as (Dincer and Rosen, 2007)

$$\dot{E}x_Q - \dot{E}x_W = \sum \dot{E}x_{in} - \sum \dot{E}x_{out} + T_0\dot{S}_{gen} \quad (3)$$

where the first and the second terms are exergy of heat and work respectively, $\dot{E}x$ is the rate of flow exergy, T_0 is the reference state temperature and the last term is entropy generation. In the above equation, each term is defined as follows:

$$\dot{E}x_{dest} = T_0\dot{S}_{gen} \quad (4)$$

$$\dot{E}x_Q = \dot{Q} \left(\frac{T-T_0}{T} \right) \quad (5)$$

$$\dot{E}x_W = \dot{W} \quad (6)$$

$$\dot{E}x_W = \dot{m} ex \quad (7)$$

In Equation (7), ex is the specific flow exergy and can be calculated using the equation below:

$$ex = (h - h_0) - T_0(s - s_0) \quad (8)$$

Applying the above mentioned general balance equations to individual system elements, energy capacity, exergy destruction rate and exergetic efficiency of each system components can be obtained as follows:

Turbine

$$\dot{W}_T = \dot{m}_1(h_1 - h_2) \quad (9)$$

$$\dot{E}x_{dest,T} = \dot{E}x_1 - \dot{E}x_2 - \dot{W}_T \quad (10)$$

$$\eta_{ex,T} = \frac{\dot{W}_T}{\dot{E}x_1 - \dot{E}x_2} \quad (11)$$

Rectifier

$$\dot{Q}_{Rec} = \dot{m}_2(h_2 - h_3) = \dot{m}_5(h_6 - h_5) \quad (12)$$

$$\dot{E}x_{dest,Rec} = \dot{E}x_2 - \dot{E}x_3 + \dot{E}x_5 - \dot{E}x_6 \quad (13)$$

$$\eta_{ex,Rec} = \frac{\dot{E}x_6 - \dot{E}x_5}{\dot{E}x_2 - \dot{E}x_3} \quad (14)$$

Condenser

$$\dot{Q}_{Con} = \dot{m}_3(h_3 - h_4) = \dot{m}_{10}(h_{10} - h_9) \quad (15)$$

$$\dot{E}x_{dest,Con} = \dot{E}x_3 - \dot{E}x_4 + \dot{E}x_9 - \dot{E}x_{10} \quad (16)$$

$$\eta_{\text{ex,Con}} = \frac{\dot{E}_{x_{10}} - \dot{E}_{x_9}}{\dot{E}_{x_3} - \dot{E}_{x_4}} \quad (17)$$

Pump

$$\dot{W}_P = \dot{m}_4(h_5 - h_4) \quad (18)$$

$$\dot{E}_{x_{\text{dest,P}}} = \dot{E}_{x_4} - \dot{E}_{x_5} + \dot{W}_P \quad (19)$$

$$\eta_{\text{ex,P}} = \frac{\dot{E}_{x_5} - \dot{E}_{x_4}}{W_P} \quad (20)$$

Vaporizer

$$\dot{Q}_{\text{vap}} = \dot{m}_1(h_1 - h_6) = \dot{m}_7(h_7 - h_8) \quad (21)$$

$$\dot{E}_{x_{\text{dest,Vap}}} = \dot{E}_{x_6} - \dot{E}_{x_1} + \dot{E}_{x_7} - \dot{E}_{x_8} \quad (22)$$

$$\eta_{\text{ex,Vap}} = \frac{\dot{E}_{x_1} - \dot{E}_{x_6}}{\dot{E}_{x_7} - \dot{E}_{x_8}} \quad (23)$$

The isentropic efficiency of the turbine and pump can be expressed as;

$$\eta_{\text{is,T}} = \frac{h_1 - h_2}{h_1 - h_{2\text{is}}} \quad (24)$$

$$\eta_{\text{is,P}} = \frac{h_{5,\text{is}} - h_4}{h_5 - h_4} \quad (25)$$

The energy efficiency of the geothermal power plant can be written as;

$$\eta_{\text{en}} = \frac{\dot{W}_{\text{net}}}{\dot{Q}_{\text{vap}}} \quad (26)$$

The exergetic performance of the power plant can be evaluated calculated using the equation below:

$$\eta_{\text{ex}} = \frac{\dot{W}_{\text{net}}}{\dot{E}_{x_7} - \dot{E}_{x_8}} \quad (27)$$

5. Results and Discussion

For the performance analysis of the geothermal assisted transcritical power cycle for different supercritical fluids, data for an actual geothermal plant were used. During the calculations, the data provided in Table 3 were used with assumptions explained previously. The calculations were made for a constant geothermal thermal power of 34381 kW for all working fluids. In addition, minimum pinch point temperature was calculated as 7.98°C for R41 during the analysis of the rectifier and it was within the limits. For all other analyses, it was higher than the considered value. Since the supercritical fluids' critical properties differ from each other, the condensing temperature was assumed to be 6 °C lower than the critical temperature for all fluids for consistency. In addition, the cooling water temperature was assumed to be 6 °C higher than the corresponding wet bulb temperature since the water was cooled in the cooling tower. Based on the design parameters, the estimated pressure values of each working were fluid were given in Figure 4. It is obvious from the figure that, during the calculations, the highest operation pressure belongs to R744, followed by R41 and R170. The operation pressure is very important during the system design since higher pressure values result in the construction of the system with higher durability.

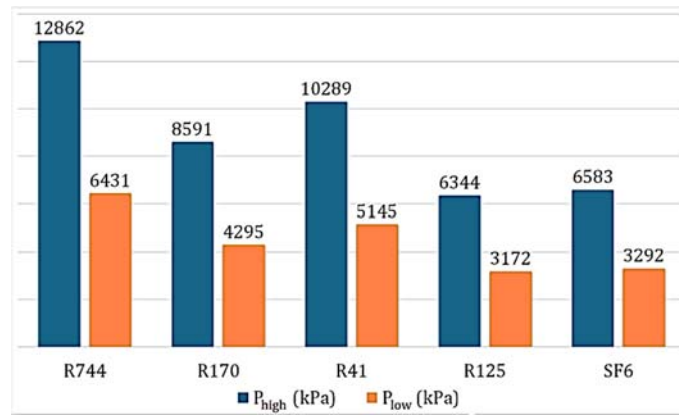


Figure 4. High and low operating pressure values of transcritical Rankine cycle for different supercritical fluids

According to the calculations, the properties of the working fluids for the state points are listed in Table 4 for the geothermal based power cycle by referring to Figure 2. The tabulated data includes the actual values for geothermal water and calculated results for the working fluids. The corresponding enthalpy and entropy values were determined using EES software as mentioned before while the specific exergy and exergy rate of each state were calculated using equations explained in the previous section.

Table 4. Thermophysical property data of state points under the specified design conditions

State	Fluid	T (°C)	P (kPa)	m (kPa)	h (kJ/kg)	s (kJ/kgK)	ex (kJ/kg)	Ex (kW)
0	R744	18	101.3	-	-6.871	-0.02233	-	-
	R170				-14.13	-0.0458		
	R41				618.4	3.204		
	R125				356.2	1.693		
	Sf6				11.58	0.04102		
	water				75.56	0.2675		
1	R744	146	12862	262.2	45.22	-0.7252	256.7	67307
	R170		8591	181	145.2	-0.7244	356.9	64582
	R41		10289	205.2	670	2.332	305.6	62708
	R125		6344	588.7	431.3	1.654	86.15	50716
	Sf6		6583	721.1	83.94	0.03072	75.36	54343
	water		75.56	0.2675				
2	R744	89.96	6431	262.2	12.32	-0.7023	217.2	56939
	R170	105.6	4295	181	95.8	-0.6916	298	53922
	R41	91.15	5145	205.2	630.7	2.359	258.4	53015
	R125	116.6	3172	588.7	419.7	1.662	72.42	42637
	Sf6	120.1	3292	721.1	73.55	0.03735	63.05	45464
	water	75.56	0.2675					
3	R744	48.01	6431	262.2	-47.63	-0.8784	208.5	54657
	R170	52.08	4295	181	-42.89	-1.087	274.4	49664
	R41	59.22	5145	205.2	562.7	2.163	247.4	50761
	R125	78.65	3172	588.7	375.3	1.542	62.97	37068
	Sf6	62.72	3292	721.1	21.59	-0.1057	52.73	38024
	water	75.56	0.2675					
4	R744	24.98	6431	262.2	-232.4	-1.492	202.3	53044
	R170	26.17	4295	181	-309.5	-1.966	263.6	47696
	R41	38.13	5145	205.2	324.9	1.407	230	47188
	R125	60.02	3172	588.7	290.5	1.29	51.59	30372
	Sf6	39.57	3292	721.1	-46.67	-0.321	47.16	34007
	water	75.56	0.2675					
5	R744	37.52	12862	262.2	-222.2	-1.487	211.1	55341
	R170	38.69	8591	181	-294	-1.958	276.9	50111
	R41	51.24	10289	205.2	337	1.412	240.4	49321
	R125	69.17	6344	588.7	294.5	1.291	55.1	32436
	Sf6	48.39	6583	721.1	-43.44	-0.3195	49.96	36025
	water	75.56	0.2675					
6	R744	54.22	12862	262.2	-162.2	-1.299	216.4	56735
	R170	64.79	8591	181	-155.3	-1.532	291.6	52771
	R41	66.92	10289	205.2	405	1.617	248.9	51065
	R125	91.75	6344	588.7	338.9	1.417	62.99	37083
	Sf6	81.23	6583	721.1	8.526	-0.1661	57.25	41283
	water	75.56	0.2675					
7	water	156	940	165	658.5	1.902	107	17651
8	water	78.4	940	165	328.9	1.056	23.9	3944
9	water	18.14	101.3	1180	76.16	0.2696	0.000145	0.1711
10	water	27.95	101.3	1180	117.2	0.4082	0.6959	821.2

Figure 5 shows the results of the energy analysis for different working fluids. According to results, the maximum net power generation was obtained for supercritical fluid R170 with 6125 kW followed by R744, R41, SF6, and R125. With parallel to this, the maximum energy efficiency was calculated for R170. In Figure 6, the result of exergy analysis is given. On contrary to the result of the energy analysis, the highest exergy destruction rate was calculated for R125 followed by SF6 and R41. The result shows that with an exergy input of 13707 kW, 8397 kW of exergy is destroyed for transcritical cycle using R125 which corresponds to the lowest exergy efficiency within the working fluids with a value of 32.38 %.

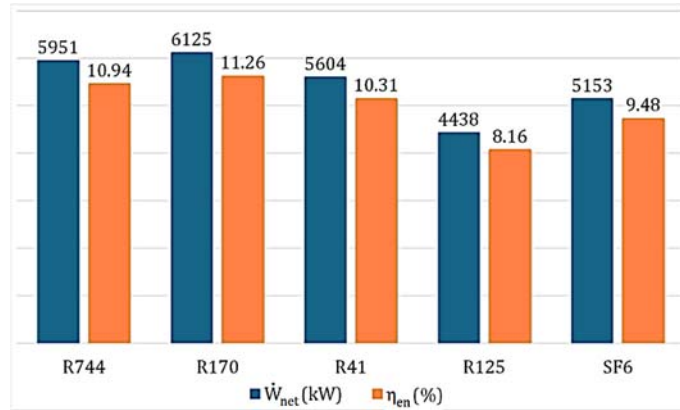


Figure 5. Energy analysis result of the geothermal based power cycle

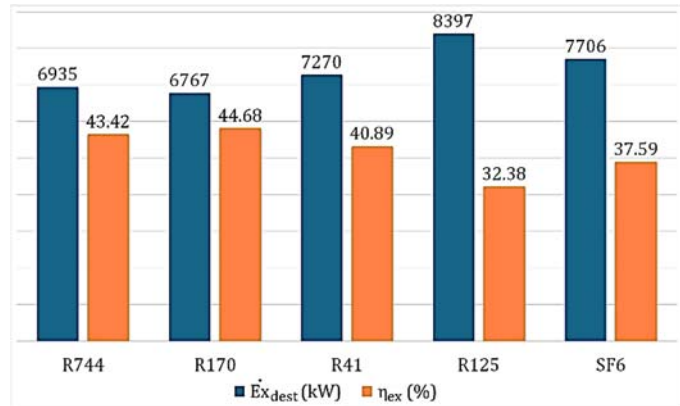


Figure 6. Exergy analysis result of the geothermal based power cycle

The exergy destruction rate and relative exergy destruction of individual system components are listed in Table 5 with component exergy efficiencies. As can be seen from the table, maximum relative irreversibility is found to be vaporizer with 45.19% for R744, and with 28% for R170. For the other supercritical fluids, the maximum relative irreversibility is calculated for the condenser. Actually, it is obvious that all the highest irreversibility rates occur in the heat exchangers due to the heat transfer process over a finite temperature difference. For the turbine and pump, the exergy destruction occurs owing to the friction losses and the unideal adiabatic expansion or compression.

Table 5. Exergy efficiency and exergy destruction rate and relative irreversibility of each system component

	R744			R170			R41			R125			SF6		
	η_{ex} (%)	$\dot{E}x_{dest}$ (kW)	RI (%)	η_{ex} (%)	$\dot{E}x_{dest}$ (kW)	RI (%)	η_{ex} (%)	$\dot{E}x_{dest}$ (kW)	RI (%)	η_{ex} (%)	$\dot{E}x_{dest}$ (kW)	RI (%)	η_{ex} (%)	$\dot{E}x_{dest}$ (kW)	RI (%)
Turbine	83.18	1744	25.15	83.79	1728	25.53	83.25	1624	22.33	84.22	1275	15.18	84.33	1391	18.05
Rectifier	61.09	887.8	12.80	62.46	1598	23.61	77.34	510.7	7.02	83.45	921.7	10.97	70.68	2181	28.30
Pump	77.13	376	5.42	86.17	393.6	5.82	84.95	332.1	4.56	99.46	302	3.59	95.28	317.3	4.11
Vaporizer	85.93	3134	45.19	85.98	1895	28.00	86.53	2063	28.37	87.23	73.92	0.88	86.41	647.6	8.40
Condenser	50.89	792.3	11.42	41.44	1152	17.02	23.3	2740	37.69	13.02	5825	69.36	21.1	3169	41.12

In the second stage of the study, a parametrical analysis was carried out for determining the effect of pressure ratio, i.e. turbine inlet pressure, on system performance. For this aim, the pressure ratio varied 1.2 and 2.6 while the other parameters were kept constant. Figure 7 shows the variation of net power generation with pressure ratio. As seen from the figure, with the increasing pressure ratio, net power generation increases for all working

fluids. However, near the pressure ratio of 2, the increment ratio starts to drop by a small amount and after 2.6, there is no increment observed in the power generation. This mainly due to the pump energy consumption increases with the pressure ratio. In Figure 8, the variation in energy efficiency against the pressure ratio is given for different working fluids. Again, energy efficiency shows the same trend with power generation.

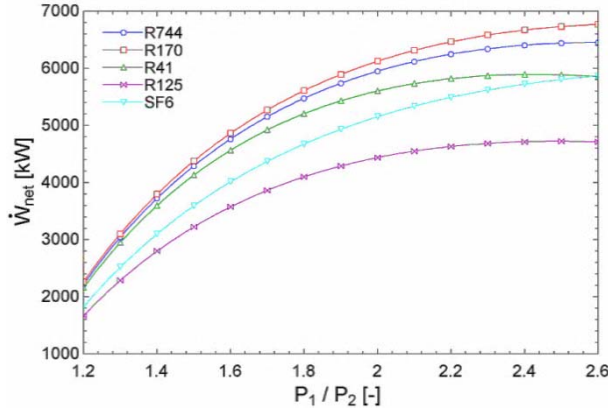


Figure 7. Variation of net power generation with pressure ratio

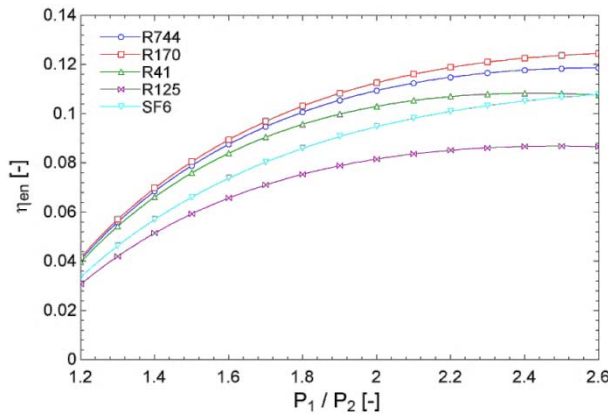


Figure 8. Variation of energy efficiency with pressure ratio

For the effect of pressure ratio on the second law characteristics of the system, Figures 9 and 10 were plotted for exergy destruction rate and exergy efficiency, respectively. While the pressure ratio increases, the exergy destruction rate decreases for all supercritical fluids. However, near the pressure ratio of 2.6, the exergy destruction rate starts to follow a straight line which means no change in the destruction. The pressure ratio of 2.6 corresponds to a turbine inlet pressure of 16721 kPa, 11168 kPa, 13376 kPa, 8247 kPa and 8558 kPa for R744, R170, R41, R125, and SF6, respectively. On contrary to this, exergy efficiency increases for all fluids. These results mainly depend on the thermophysical properties of the working fluids.

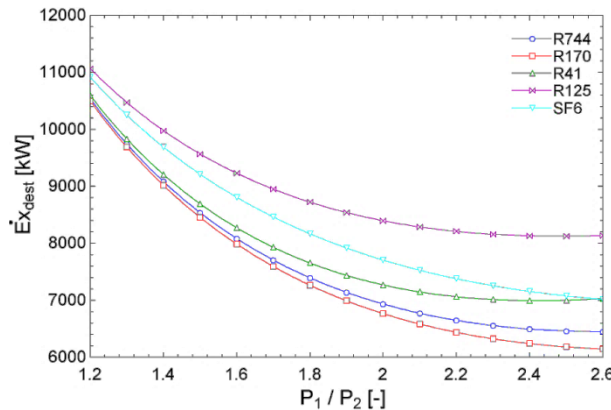


Figure 9. Variation of exergy destruction rate with pressure ratio

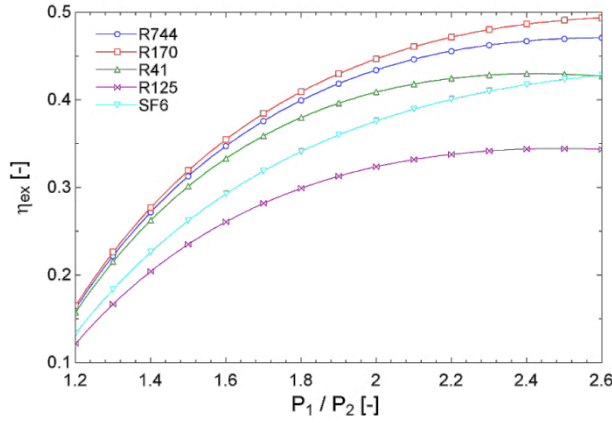


Figure 10. Variation of exergy efficiency with pressure ratio

Another important parameter that affects the system performance is the turbine inlet temperature. For this aim, parametric analyses were carried out to investigate the effect of T_1 with net power generation, energy efficiency, exergy destruction, and exergy efficiency. Figure 11 shows the net power generation against the turbine inlet temperature. As seen from the figure, R125 has the lowest power generation but it is affected by the temperature more than the others. Figure 12 shows the energy efficiency variation with the turbine inlet temperature. For all working fluids, energy efficiency increases with the temperature. However, the increment slope for R170, R744, and R41 is nearly constant.

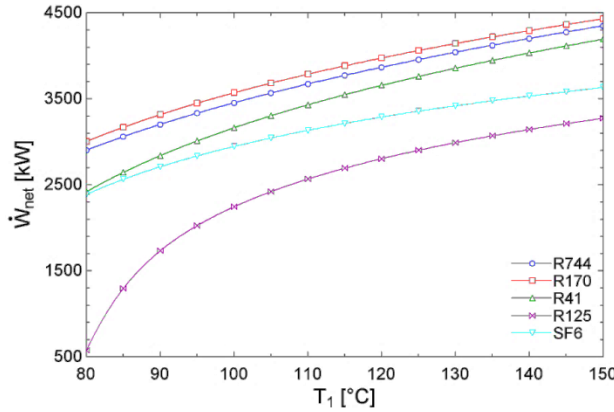


Figure 11. Variation of net power generation with turbine inlet temperature

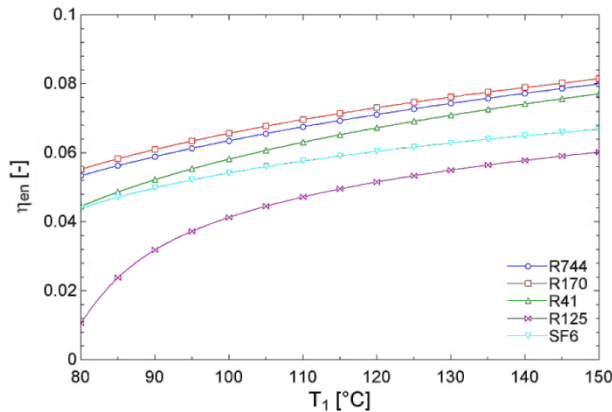


Figure 12. Variation of energy efficiency with turbine inlet temperature

The effect of turbine inlet temperature on the exergy destruction and exergy efficiency is given in Figures 13 and 14. As seen from Figure 14, while the temperature increases, the exergy destruction decreases for all working fluids. The highest destruction ratio occurs for R125 between 80-100 °C. After this temperature range, the decrement ratio becomes nearly constant for all fluids. In the same manner, exergy efficiency increases with the turbine inlet temperature as seen in Figure 15. The highest exergy efficiency belongs to R170 with 21.92 % at 80

°C. When the turbine inlet temperature increases to 150 °C, the exergy efficiency increases to a value of 32.32 % for R170 which corresponds to an increment ratio of nearly 47 %.

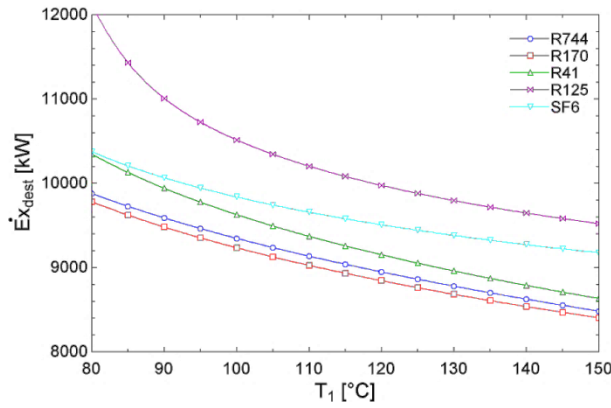


Figure 13. Variation of exergy destruction rate with turbine inlet temperature

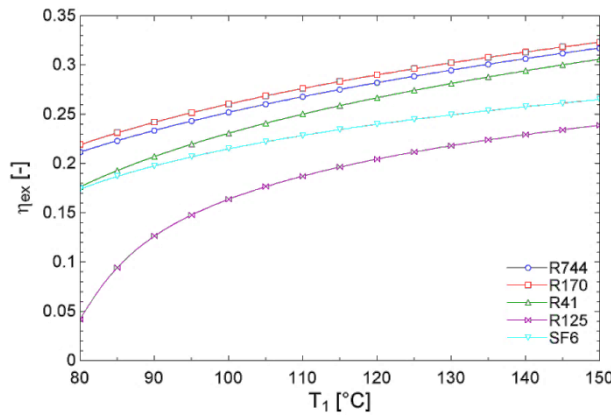


Figure 14. Variation of exergy efficiency with turbine inlet temperature

6. Conclusions

Performance evaluation of a transcritical Rankine cycle driven by low-grade geothermal energy was carried for different supercritical fluids. Calculations were made for a geothermal water extraction temperature of 156 °C, which was taken from an actual power plant. Analyses were made for five different supercritical fluids. From the results, it was observed that the highest power generation rate was calculated for the system using R170 with a net turbine power of 6125 kW and an energy efficiency of 11.26 %. After R170, the best working was found to be R744, followed by R41, SF6, and R125. R170 and R744 are both natural and non-toxic working fluids with zero ODP and very low GWP. They both have a lower critical temperature which is around 30 °C. However, R170 is flammable while R744 is non-flammable, therefore special attention has to be given for the utilization of R170. According to the second law analysis, the highest exergy destruction rate was occurred in the cycle using R125 with a value of 8397 kW followed by SF6, R41, R744, and R170. These results, show that, among the supercritical working fluids investigated in the present study, R170 and R744 have great potential for transcritical power generation applications utilizing low-grade thermal energy. In addition, parametric analyses were carried out in order to determine the effects of pressure ratio and turbine inlet temperature on the system performance such as power generation, exergy destruction, energy efficiency, and exergy efficiency. It was observed that, for all working fluids, the power generation rate was increased with the pressure ratio and turbine inlet temperature while the exergy destruction rate decreased. Consequently, due to their low critical points, supercritical working fluids have got some advantages to be utilized in thermodynamic cycles. However, further research needs to be done to investigate the utilization of these fluids for different system parameters such as ambient temperature, cooling water temperature, environmental concerns, economic criteria, etc. The findings of this study give brief information about utilizing the supercritical fluids in a low-grade geothermal based power transcritical power cycle.

Nomenclature

ex specific exergy (kJ/kg)

\dot{E}_x	exergy rate (kW)
h	specific enthalpy (kJ/kg)
\dot{m}_i	mass flow rate (kg/s)
\dot{Q}	heat energy rate (kW)
P	pressure (kPa)
s	specific entropy (kJ/kgK)
\dot{S}	entropy rate (kW/K)
T	temperature (°C)
\dot{W}	work rate (kW)

Greek letters

η_{en}	energy efficiency
η_{ex}	energy efficiency
ε	heat exchanger effectiveness

Subscripts

c	critical
Con	condenser
$dest$	destroyed
gen	generation
in	inlet stream
is	isentropic
out	outlet stream
P	pump
Rec	rectifier
T	turbine
Vap	vaporizer
wb	wet bulb
0	reference state

Acronyms

ORC	organic Rankine cycle
sCO ₂	supercritical carbondioxide
tCO ₂	transcritical carbondioxide
ODP	ozone depletion potential
GWP	global warming potential

References

- Abdolalipouradl, M., Khalilarya, S., Jafarmadar, S., (2019). Exergoeconomic analysis of a novel integrated transcritical CO₂ and Kalina 11 cycles from Sabalan geothermal power plant. *Energy Conversion and Management*, 195, 420–435.
- Ahmadi, M.H., Mehrpooya, M., Abbasi, S., Pourfayaz, F., Bruno, J.C., (2017). Thermo-economic analysis and multi-objective optimization of a transcritical CO₂ power cycle driven by solar energy and LNG cold recovery. *Thermal Science and Engineering Progress*, 4, 185-196.
- ASHRAE (2009). *Ashrae Handbook Fundamentals*. American Society of Heating, Refrigerating and Air-Conditioning Engineers, 880pp.
- Babatunde A.F., Sunday, O.O. (2018). A Review of Working Fluids for Organic Rankine Cycle (ORC) Applications. *IOP Conf. Ser.: Mater. Sci. Eng.* 413, 012019.
- Bandean, D.C., Smolen, S., Cieslinski, J.T. (2011). Working fluid selection for Organic Rankine Cycle applied to heat recovery systems. *World Renewable Energy Congress*, 8-13 May 2011, Linköping Sweden, 772-779.
- Cengel, Y.A., Boles, M.A. (2006). *Thermodynamics: an engineering approach*. McGraw-Hill, New York,

- Chen, Y., Lundqvist, P., Johansson, A., Platell, P., (2006). A comparative study of the carbon dioxide transcritical power cycle compared with an organic rankine cycle with R123 as working fluid in waste heat recovery. *Applied Thermal Engineering*, 26(17–18), 2142-2147.
- Chen, Y., Lundqvist, P., Platell, P., (2005). Theoretical research of carbon dioxide power cycle application in automobile industry to reduce vehicle's fuel consumption. *Applied Thermal Engineering*, 25(14–15), 2041-2053.
- Dincer, I., Rosen, M.A. (2007). *Exergy: Energy, Environment and Sustainable Development*. Elsevier Science.
- Fiaschi, D., Manfrida, G., Rogai, E., Talluri, L., (2017). Exergoeconomic analysis and comparison between ORC and Kalina cycles to exploit low and medium-high temperature heat from two different geothermal sites. *Energy Conversion and Management*, 154, 503–516.
- Heberle, F., Hofer, M., Brüggemann, D. (2017a). A Retrofit for Geothermal Organic Rankine Cycles based on Concentrated Solar Thermal Systems. *Energy Procedia*. 129, 692-699.
- Heberle, F., Hofer, M., Ürlings, N., Schröder, H., Anderlohr, T., Brüggemann, D. (2017b). Techno-economic analysis of a solar thermal retrofit for an air-cooled geothermal Organic Rankine Cycle power plant. *Renewable Energy*, 113, 494-502
- Jumel, S., Feidt, M., Le, V.L., Kheiri, A. (2012). Working fluid selection and performance comparison of subcritical and supercritical organic Rankine cycle (ORC) for low temperature waste heat recovery. *ECEEE 2012 Summer Study on Energy Efficiency in Industry*, 559-569.
- Kajurek, J., Rusowicz, A., Grzebielec, A., Bujalski, W., Futyma, K., Rudowicz, Z. (2019). Selection of refrigerants for a modified organic Rankine cycle. *Energy*, 168, 1-8.
- Karellas, S., Schuster, A. (2008). Supercritical Fluid Parameters in Organic Rankine Cycle Applications. *Int. J. of Thermodynamics*, 11(3), 101-108.
- Karimi, S., Mansouri, S., (2018). A comparative profitability study of geothermal electricity production in developed and developing countries: Exergoeconomic analysis and optimization of different ORC configurations. *Renewable Energy*, 115, 600-619.
- Klein, S.A. (2018). *Engineering Equation Solver. (EES). F-Chart*.
- Li, H., Yang, Y., Cheng, Z., Sang, Y., Dai, Y., (2018). Study on off-design performance of transcritical CO₂ power cycle for the utilization of geothermal energy. *Geothermics*, 71, 369–379.
- Liu, B.T., Chien, K.H., Wang, C.C. (2004). Effect of working fluids on organic Rankine cycle for waste heat recovery. *Energy*, 29(8), 1207-1217.
- Meng, F., Wang, E., Zhang, B., Zhang, F., Zhao, C., (2019). Thermo-economic analysis of transcritical CO₂ power cycle and comparison with Kalina cycle and ORC for a low-temperature heat source. *Energy Conversion and Management*, 195, 1295-1308.
- Moloney, F., Almatrafi, E., Goswami, D.Y. (2017). Working fluid parametric analysis for regenerative supercritical organic Rankine cycles for medium geothermal reservoir temperatures. *Energy Procedia*, 129, 599-606.
- Nami, H., Nemati, A., Fard, F.J., (2017). Conventional and advanced exergy analyses of a geothermal driven dual fluid organic Rankine cycle (ORC). *Applied Thermal Engineering*, 122, 59–70.
- Radulovic, J. (2015). Utilisation Of Fluids With Low Global Warming Potential In Supercritical Organic Rankine Cycle. *Journal of Thermal Engineering*, 1(1), 24-30.
- Schuster, A., Karellas, S., Aumann, R. (2010). Efficiency optimization potential in supercritical Organic Rankine Cycles. *Energy*, 35(2), 1033-1039.

- Sun, J., Liu, Q., Duan, Y. (2018). Effects of evaporator pinch point temperature difference on thermo-economic performance of geothermal organic Rankine cycle systems. *Geothermics*, 75, 249-258.
- Song, C., Gu, M., Miao, Z., Liu, C., Xu, J., (2019). Effect of fluid dryness and critical temperature on trans-critical organic Rankine cycle. *Energy*, 174, 97-109.
- Thanganadar, D., Asfand, F., Patchigolla, K., (2019). Thermal performance and economic analysis of supercritical Carbon Dioxide cycles in combined cycle power plant. *Applied Energy*, 255, 113836.
- Thurairajaab, K., Wijewardane, A., Jayasekara, S., Ranasinghe, C., (2019). Working Fluid Selection and Performance Evaluation of ORC. *Energy Procedia*, 156, 244-248.
- Wang, X., Levy, E.K., Pan, C., Romero, C.E., Banerjee, W., Rubio-Maya, C., Pan, L. (2019). Working fluid selection for organic Rankine cycle power generation using hot produced supercritical CO₂ from a geothermal reservoir. *Applied Thermal Engineering*, 149, 1287-1304.
- Wang, J., Sun, Z., Dai, Y., Ma, S., (2010). Parametric optimization design for supercritical CO₂ power cycle using genetic algorithm and artificial neural network. *Applied Energy*, 87(4), 1317-1324.
- Zhang, C., Lin, J., Tan, Y. (2019). A theoretical study on a novel combined organic Rankine cycle and ejector heat pump. *Energy*, 176, 81-90.
- Wang, X., Levy, E.K., Pan, C., Romero, C.E., Banerjee, A., Maya, C.B., Pan, L., (2019). Working fluid selection for organic Rankine cycle power generation using hot produced supercritical CO₂ from a geothermal reservoir. *Applied Thermal Engineering*, 149, 1287-1304.
- Xu, W., Deng, D., Zhang, Y., Zhao, D., Zhao, L., (2019). How to give a full play to the advantages of zeotropic working fluids in organic Rankine cycle (ORC). *Energy Procedia*, 158, 1591-1597.
- Yang, Y., Huo, Y., Xia, W., Wang, X., Zhao, P., Dai, Y., (2017). Construction and preliminary test of a geothermal ORC system using geothermal resource from abandoned oil wells in the Huabei oilfield of China. *Energy*, 140, 633-645.
- Yu, H., Kim, D., Gundersen, T., (2019). A study of working fluids for Organic Rankine Cycles (ORCs) operating across and below ambient temperature to utilize Liquefied Natural Gas (LNG) cold energy. *Energy*, 167, 730-739.